

Time-dependent Density Functional calculation of e-H scattering

Meta van Faassen,¹ Adam Wasserman,² Eberhard Engel,³ Fan Zhang,¹ and Kieron Burke⁴

¹*Department of Chemistry and Chemical Biology, Rutgers University,
610 Taylor Road, Piscataway, NJ 08854-8087, USA*

²*Department of Chemistry and Chemical Biology, Harvard University,
12 Oxford St., Cambridge Massachusetts 02138, USA*

³*Center for Scientific Computing, JW Goethe-Universität Frankfurt,
Max-von-Laue-Straße 1, D-60438 Frankfurt/Main, Germany*

⁴*Department of Chemistry, University of California, Irvine, CA 92697, USA*

(Dated: November 1, 2018)

Phase shifts for single-channel elastic electron-atom scattering are derived from time-dependent density functional theory. The H^- ion is placed in a spherical box, its discrete spectrum found, and phase shifts deduced. Exact-exchange yields an excellent approximation to the ground-state Kohn-Sham potential, while the adiabatic local density approximation yields good singlet and triplet phase shifts.

PACS numbers: 31.15.Ew, 31.10.+z, 34.80.Bm, 31.25.Jf

Modern density functional theory (DFT) [1, 2, 3] has proven very successful in quantum chemistry and solid-state physics. The time-dependent formulation, TDDFT [4], extends this success to excited-state properties [5]. Thus, excitation energies and oscillator strengths of electronic transitions of atoms, molecules, and clusters are now routinely calculated via TDDFT within, e.g., the adiabatic local density approximation (ALDA) [6]. But such calculations are almost exclusively for optical response to either weak [5] or strong [7] fields.

The problem of calculating low-energy elastic electron scattering from atoms and molecules is demanding, and solving the Schrödinger equation for continuum states of polyatomic molecules can be expensive. However, such solutions are needed for the emergent field of electron-impact chemistry [8], especially since recent experiments show that low energy electrons can cleave DNA [9, 10]. Through efficient use of R-matrix theory, calculations within static exchange (amounting to scattering from an effective one-body potential) have been performed for a single DNA base [11]. A TDDFT approach could prove highly useful here, allowing the incorporation of correlation effects with little additional cost beyond the original scattering calculation.

With this ultimate goal in mind, we demonstrate a simple method for using TDDFT to calculate phase shifts. We find the continuum states of the $N + 1$ -electron problem, where the target has N electrons. Our method is extremely practical in spherical cases, such as atoms. It is based on a little-used formula [12, 13, 14, 15, 16] (exact for finite-ranged potentials) that relates the phase shift of the continuum problem to discrete energies of the same potential, but placed inside a box whose edge is beyond the range of the potential. This formula bypasses many of the complications of our original work [17], as now we need only find bound-bound transition energies, where TDDFT has already proven successful. Further-

more, since our general approach requires that the $N + 1$ -electron system be bound, by putting the system in a box, our new method can be applied, at least in principle, even when the ‘ground state’ of the $N + 1$ -electron system is only a resonance.

A vital element in any DFT approach is the accuracy of approximate functionals used. In this sense, electron scattering from the H atom is a very severe test, since H^- (the $N + 1$ -electron system) is so strongly correlated. The underlying ground-state Kohn-Sham (KS) potential is crucial to any TDDFT calculation, especially for atoms, and is known essentially exactly for H^- [18]. We find that exact-exchange, as calculated in an optimized effective potential (OEP) code, yields very accurate KS phase-shifts, i.e., very close to those of the known exact KS potential. Next, we show that the ALDA, the workhorse of TDDFT, yields very good shifts for both singlet and triplet (TD-spin-DFT) scattering. Thus, we demonstrate that a simple formalism allows scattering calculations from TDDFT; that modern approximations yield sufficiently accurate ground-state potentials; and that standard TDDFT approximations are sufficiently accurate. We perform the first such calculation on the prototype target, the H atom.

We begin with some exact observations about scattering from a potential. Consider a spherical potential that has a finite range, i.e., $v(r) = 0$ beyond some radius R_c . Now imagine inserting a hard wall at any $R_b > R_c$, not necessarily far beyond R_c , and solving for the bound states. Any such solution is in fact a solution to the original scattering problem that happens to have a node right at R_b . Study of the wavefunction between R_c and R_b to identify the phase shift yields:

$$\tan(\delta_{l\alpha}) = -j_l(k_\alpha R_b)/\eta_l(k_\alpha R_b) \quad (1)$$

where j_l and η_l are the two free-space solutions to the radial Schrödinger equation, i.e., the spherical Bessel and

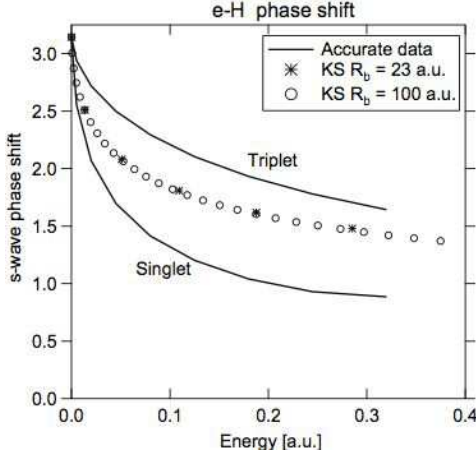


FIG. 1: Accurate quantum chemical singlet and triplet s-phase shifts [19], together with the KS values, calculated with a wall at 23 a.u. and at 100 a.u..

von Neumann functions, $k_\alpha = \sqrt{2E_\alpha}$, and E_α is the α -th eigenenergy. For s-wave scattering, Eq. (1) reduces to:

$$\delta_\alpha = -k_\alpha R_b + \alpha\pi \quad (l=0) \quad (2)$$

The phase shifts are only determined modulo π , but we have added $\alpha\pi$, the free-particle value of $k_\alpha R_b$, so that all shifts are relative to 0. For any given l and R_b , this method yields the phase shift at a discrete set of energies. For a fixed potential, starting from *any* R_b value, R_0 , one can continuously increase R_b to about $2R_0$ and generate δ at *all* energies above a minimum $E_{\min} = \frac{1}{2}[(\pi - \delta_n)/R_b]^2$, where R_b is the largest box used. Usually R -matrix theory is more convenient, as it does not require the wavefunction to have a node at the box radius, and so all energies can be found with just one value of R_b . But it relies on knowing the logarithmic derivative of the wavefunction at R_b , which is not available in TDDFT.

To illustrate the method, and show how useful the exact ground state KS potential is, in Fig. 1 we plot accurate quantum calculations for both singlet and triplet elastic scattering from hydrogen [19]. We also plot the result of potential scattering from the exact ground state KS potential of H^- . This was found by Umrigar *et al.* [18], from an extremely accurate quantum Monte-Carlo calculation for the ground state of H^- , calculating the density, and finding $v_s(\mathbf{r})$ by inverting the KS equation. We obtained the positive orbital energies (necessary to evaluate Eq. (2)) from a well-established fully numerical spherical DFT code, which includes the optimized effective potential method (OEP) and has been supplemented by the option to insert a hard-wall at a distance R_b from the origin[20].

The KS phase shift fits between the two curves, just as the pure KS orbital energy differences lie between singlet and triplet excitations for He [21, 22]. The calculations at two values of R_b demonstrate the results are indepen-

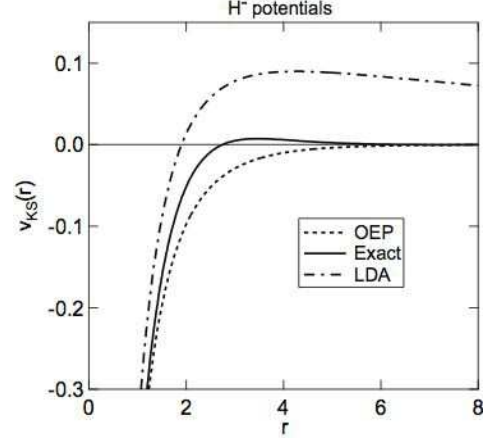


FIG. 2: The exact, exact-exchange, and LDA KS-potentials for H^- .

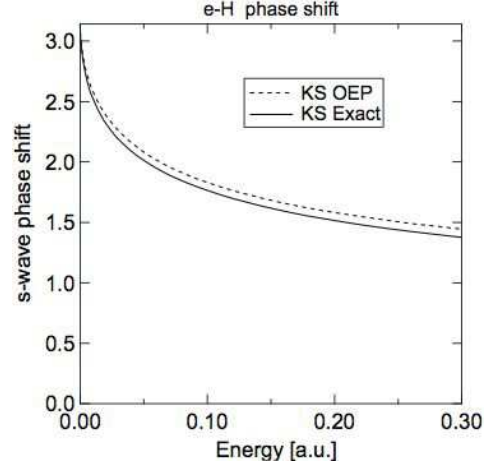


FIG. 3: The s-wave phase shifts for the exact and exact-exchange KS potentials for H^- .

dent of R_b . We choose the wall far from the origin to ensure the self-consistent *ground-state* results are not affected by its position and to approach zero energy, but we emphasize the fact that Eq. (2) is exact for any $R_b > R_c$.

Obviously, the decay of the ground-state KS potential is crucial to the accuracy of this method, and in any practical application, the exact KS potential is unavailable. Therefore we study the behavior of two approximate potentials, exact-exchange (OEP) and the local density approximation (LDA). In Fig. 2, we plot both the exact and approximate KS potentials for H^- . The LDA potential is far too shallow, a well-known failing of most commonly-used approximations to ground-state DFT. The true self-consistent LDA potential does not support any bound states, so to obtain the potential we put the system in a large box, forcing the states to be bound [23]. Thus, the LDA potential is utterly unsuitable for this type of calculation. On the other hand, the exact-exchange potential decays correctly as $r \rightarrow \infty$, missing only the small

positive correlation potential for small r . Many modern R -matrix based methods start with the nuclear potential and the pure electrostatic (i.e., Hartree) potential, and then add the LDA exchange potential from DFT, i.e., the Slater contribution that decays exponentially, as $n^{1/3}(r)$. Since this potential misses the correct asymptotic behavior, $v_{\text{xc}}(r) \rightarrow -1/r$, a ‘polarization’ potential must be added [24]. Our KS potentials, either exact or exact-exchange, already have the correct asymptotic behavior, i.e., they contain the polarization potential. Without this feature, our KS potentials would have the wrong asymptotic behavior, and would not be long-ranged for neutral atoms. In Fig. 3, we plot the scattering from the exact and exact-exchange potentials, demonstrating that exact-exchange, as is now available in many codes [25], is perfectly adequate for this purpose.

To go even further, e.g. to account for singlet-triplet splitting, we must use TDDFT. Within the formalism of TDDFT within linear response we can, in principle, obtain the true singlet and triplet excitation energies, and thus the phase shifts. We label all single-particle excitations from the ground to unoccupied excited states via $q = (i, a)$, where i implies occupied, a implies unoccupied, and define $\Phi_{q\sigma}(\mathbf{r}) = \phi_{i\sigma}^*(\mathbf{r})\phi_{a\sigma}(\mathbf{r})$, where σ is a spin index and $\phi_i(\mathbf{r})$ is an eigenstate of the ground state $v_{\text{S}}(\mathbf{r})$. Casida [26] cast the TDDFT response equations as a eigenvalue equation

$$\sum_{q'} \tilde{\Omega}_{qq'\sigma'\sigma}(\omega) a_{q'\sigma} = \omega^2 a_{q\sigma}, \quad (3)$$

where

$$\begin{aligned} \tilde{\Omega}_{qq'\sigma'\sigma}(\omega) = & \omega_{q\sigma}^2 \delta_{qq'} \delta_{\sigma\sigma'} \\ & + 2\sqrt{\omega_{q\sigma}\omega_{q'\sigma'}} \langle q\sigma | f_{\text{HXC}}^{\sigma\sigma'}(\omega) | q'\sigma' \rangle. \end{aligned} \quad (4)$$

and $\langle q\sigma | f_{\text{HXC}}^{\sigma\sigma'}(\omega) | q'\sigma' \rangle$ is the matrix element of the Hartree-XC kernel in the set of functions $\Phi_{q\sigma}(\mathbf{r})$. We also defined $\omega_{q\sigma} = \epsilon_{i\sigma} - \epsilon_{a\sigma}$, where $\epsilon_{i\sigma}$ is the KS orbital energy of state i with spin σ . The XC kernel is the functional derivative of the XC potential in TDDFT [5, 7] and we assume the frequency independent ALDA kernel in the following. The $\tilde{\Omega}$ -matrix can be split in separate singlet and triplet $\tilde{\Omega}$ -matrices [26]. Solving Eq. (3) therefore yields predictions of both singlet and triplet transition frequencies, ω . In order to perform these calculations we have added subroutines to evaluate the matrix elements needed for a TDDFT calculation. Since the system studied is small, we exactly diagonalize the $\tilde{\Omega}$ -matrix.

In Fig. 4, we show the results obtained from a TDDFT ALDA calculation, but using the OEP ground-state potential. Apart from the full results we also show results obtained with the single-pole approximation (SPA), which ignores the off-diagonal matrix elements in Eq. (4) [27]. The SPA is analogous to the distorted-wave Born approximation used in earlier work, which worked

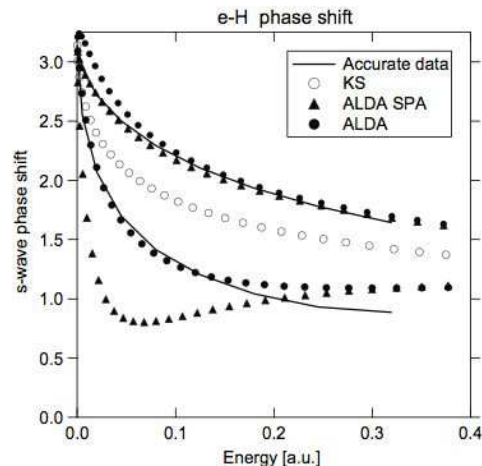


FIG. 4: Singlet and triplet TDDFT curves from an SPA and full ALDA calculation, together with the KS values and accurate quantum chemical data from Ref. [19]. The ground state KS potential is exact-exchange. The wall location in all calculations is at 100 a.u.

TABLE I: TDDFT s-wave scattering lengths.

	Singlet a	Triplet a
Accurate data ^a	5.97	1.77
ALDA SPA	9.7	1.8
ALDA	5.6	2.0 ^b

^aAccurate variational calculations from [19]

^bThis is the value as obtained from our tangent approximation as explained in the text

well for electron scattering from He^+ [17], but fails badly for H. In Fig. 4 the SPA is indeed a poor approximation to the full singlet curve, especially at low energies. For the triplets, on the other hand, we obtain excellent results that are on top of the reference values.

If we now look at the full calculation we see that including the off-diagonal matrix elements considerably improves the singlet values giving results very close to the reference data. For the triplet the results only change for smaller energies where the values are too big and there is a small ‘bump’ close to $E = 0$. We believe this bump to be unphysical, due to coupling among transitions being treated incorrectly by our approximate XC-kernel, as $E \rightarrow 0$. This suspicion is reinforced by the fact that in this region, the full ALDA triplet results depend on the position of the wall, and so cannot be trusted. However, similar effects were found with other common kernels, such as exact exchange, so we believe some delicate behavior of the XC kernel is required to avoid this artifact.

To quantify results for low energies, the scattering length is defined by the effective range expansion,

$$k^{2l+1} \cot \delta_l(k) \underset{k \rightarrow 0}{=} -\frac{1}{a_l} + \frac{1}{2} r_{el} k^2 + O(k^4), \quad (5)$$

where a_l is the scattering length and r_{el} the effective

range. Since we have no wave function, to extract a_l we must fit our data to the above expression to obtain the scattering lengths. We give a rough estimate of the expected TDDFT scattering lengths in Table I, by fitting our results for small k . As a reference, the KS scattering lengths are 4.7 for the exact potential and 4.2 for the exact-exchange potential. We report the scattering lengths we obtained from our phase shifts, or in the case of the full triplet ALDA calculation, from fitting a tangent to the curve, required to pass through π . In the triplet case, the value obtained from the fit agrees well with the reference value, as does the SPA result. Thus either method yields accurate results as $k \rightarrow 0$.

Scattering from neutrals is very different from scattering from positive ions. In the former, the $N + 1$ -electron system has a *short*-ranged potential, and so a finite cross-section, but in the latter, the KS potential is *long*-ranged, i.e., it decays as $-1/r$ for large r , and the cross-section diverges. The phase-shift is then defined relative to pure Coulomb scattering. Our general approach still applies, but Eq. (1) must be modified. If a potential deviates from $-1/r$ only for $r < R_c$,

$$\tan(\delta_\alpha) = -F_l(k_\alpha R_c)/G_l(k_\alpha R_c) \quad (6)$$

where F_l and G_l are the Coulomb scattering solutions [28]. We will report results for positive ions in future publications.

While the ALDA functional uses only input from the uniform electron gas, our results show that it gives accurate results for electron-scattering from a system that could not be further away from a homogeneous gas, the hydrogen atom. These results encourage us to continue work along these lines. We will calculate other l -values, different approximate ground-state potentials, different XC-kernels, other atoms, and ions, to gain experience in the reliability of TDDFT calculations. But we finish by considering some obstacles in applying our method to scattering from large molecules. We first note that, by converting the problem to one of discrete transitions, one needs only modify an existing electronic structure code by placing a hard wall around it, rather than use a scattering code. However, our formula is only exact if the wavefunction has a node on the hard-wall surface, which would only be true state-by-state for a non-spherical system. Much better is to use a large sphere, so that the formula is approximately true. We must also address the multichannel case. We intend applying our method to electron scattering from Be^+ next, which is a well-studied scattering example [29], and for which the exact ground-state KS potential is known [18].

We gratefully acknowledge support from NSF Grant No. CHE-0355405. MvF acknowledges The Netherlands Organization for Scientific Research (NWO) for support through a VENI grant. We also acknowledge the exact H^- KS potential from Cyrus Umrigar, and useful discus-

sions with Mike Morrison, Neepa Maitra, Chris Greene, Peter Lambropoulos and Vladimir Mandelshtam.

-
- [1] P. Hohenberg and W. Kohn, Phys. Rev. **136**, B864 (1964).
 - [2] W. Kohn and L. J. Sham, Phys. Rev. **140**, A1133 (1965).
 - [3] C. Fiolhais, F. Noguiera, and M. A. L. Marques, eds., *A Primer in Density Functional Theory* (Springer, Heidelberg, 2006), 1st ed.
 - [4] E. Runge and E. K. U. Gross, Phys. Rev. Lett. **52**, 997 (1984).
 - [5] K. Burke, J. Werschnik, and E. K. U. Gross, J. Chem. Phys. **123**, 062206 (2005).
 - [6] M. A. L. Marques, C. Ullrich, F. Noguiera, A. Rubio, K. Burke, and E. K. U. Gross, eds., *Time-Dependent Density Functional Theory* (Springer, Heidelberg, 2006).
 - [7] M. Marques and E. Gross, Annu. Rev. Phys. Chem. **55**, 427 (2004).
 - [8] G. Hanel, S. Denifl, P. Scheier, M. Probst, B. Farizon, M. Farizon, E. Illenberger, and T. D. Märk, Phys. Rev. Lett. **90**, 188104 (2003).
 - [9] B. Boudaïffa, P. Cloutier, D. Hunting, M. A. Huels, and L. Sanche, Science **287**, 1658 (2000).
 - [10] L. G. Caron and L. Sanche, Phys. Rev. Lett. **91**, 113201 (2003).
 - [11] S. Tonzani and C. H. Greene, J. Chem. Phys. **124**, 054312 (2006).
 - [12] U. Fano, Nuovo Cimento **12**, 154 (1935).
 - [13] U. Fano and C. M. Lee, Phys. Rev. Lett. **31**, 1573 (1973).
 - [14] C. M. Lee, Phys. Rev. A **10**, 584 (1974).
 - [15] B. W. Shore, J. Phys. B: Atom. Molec. Phys. **7**, 2502 (1974).
 - [16] I. M. Savukov, Phys. Rev. Lett. **96**, 073202 (2006).
 - [17] A. Wasserman, N. Maitra, and K. Burke, J. Chem. Phys. **122**, 144103 (2005).
 - [18] C. J. Umrigar and X. Gonze, in *High Performance Computing and its Application to the Physical Sciences*, edited by D. A. Browne, J. Callaway, J. P. Draayer, R. W. Haymaker, R. K. Kalia, J. E. Tohline, and P. Vashishta (World Scientific, Singapore, 1993), vol. 94.
 - [19] C. Schwarz, Phys. Rev. **124**, 1468 (1961).
 - [20] H. Jiang and E. Engel, J. Chem. Phys. **123**, 224102 (2005).
 - [21] M. van Faassen and K. Burke, J. Chem. Phys. **124**, 094102 (2006).
 - [22] M. van Faassen, Int. J. Quant. Chem. **106**, 3235 (2006).
 - [23] H. B. Shore, J. H. Rose, and E. Zaremba, Phys. Rev. B **15**, 2858 (1977).
 - [24] M. A. Morrison, Aust. J. Phys. **36**, 239 (1983).
 - [25] F. Della Sala and A. Görling, J. Chem. Phys. **115**, 5718 (2001).
 - [26] M. E. Casida, in *Recent Developments and Applications of Modern Density Functional Theory*, edited by J. M. Seminario (Elsevier, Amsterdam, 1996).
 - [27] M. Petersilka, U. J. Gossmann, and E. K. U. Gross, Phys. Rev. Lett. **76**, 1212 (1996).
 - [28] H. Friedrich, *Theoretical Atomic Physics* (Springer-Verlag, 1998), 2nd ed.
 - [29] C. H. Greene, Phys. Rev. A **23**, 661 (1981).